Received: 21 July 2016 | Accepted: 6 August 2016

DOI 10.1002/aoc.3599

WILEY Applied Organometallic Chemistry

FULL PAPER

Biological evaluation of organometallic palladium(II) complexes containing 4-hydroxybenzoic acid (3-ethoxy-2-hydroxybenzylidene)hydrazide: Synthesis, structure, DNA/protein binding, antioxidant activity and cytotoxicity

Ganesan Ayyannan[1] | Perumal Veerasamy[1] | Maruthachalam Mohanraj[1] | Gunasekaran Raja[1] | Arumugam Manimaran[2] | Marappan Velusamy[3] | Nanjan Bhuvanesh[4] | Raju Nandhakumar[4] | Chinnasamy Jayabalakrishnan[1]*

[1] Post-Graduate and Research Department of Chemistry, Sri Ramakrishna Mission Vidyalaya College of Arts and Science, Coimbatore 641020, Tamil Nadu, India

[2] Department of Chemistry, Kongunadu Arts and Science College, Coimbatore 641029, Tamil Nadu, India

[3] Department of Chemistry, North Eastern Hill University, Shillong, Meghalaya 793022, India

[4] Department of Chemistry, Karunya University, Karunya Nagar, Coimbatore 641114, Tamil Nadu, India

Correspondence
C. Jayabalakrishnan, Post-Graduate and Research Department of Chemistry, Sri Ramakrishna Mission Vidyalaya College of Arts and Science, Coimbatore – 641020, Tamil Nadu, India.
Email: drcjbstar@gmail.com

New palladium(II) complexes, [Pd(PPh_3)L] (**2**) and [Pd($AsPh_3$)L] (**3**), were synthesized using 4-hydroxybenzoic acid (3-ethoxy-2-hydroxybenzylidene)hydrazide (**1**) ligand (H_2L), and characterized using various physicochemical techniques. The molecular structures of **2** and **3** were determined using single-crystal X-ray diffraction, which reveals a square planar geometry around the palladium(II) metal ion. *In vitro* DNA binding studies were conducted using UV–visible absorption spectroscopy, emission spectroscopy, cyclic voltammetry and viscosity measurements, which suggest that the metal complexes act as efficient DNA binders. The interaction of ligand H_2L and complexes **2** and **3** with bovine serum albumin (BSA) was investigated using UV–visible and fluorescence spectroscopies. Absorption and emission spectral studies indicate that complexes **2** and **3** interact with BSA protein more strongly than the parent ligand. The free radical scavenging potential of all the synthesised compounds (**1**–**3**) was also investigated under *in vitro* conditions. In addition, the *in vitro* cytotoxicity of the complexes to tumour cells lines (HeLa and MCF-7) was examined using the MTT assay method.

KEYWORDS

antioxidant, crystal structure, cytotoxic activity, DNA/BSA binding, palladium(II) complexes

1 | INTRODUCTION

Platinum-based metallodrugs, e.g. cisplatin, oxaliplatin, carboplatin, have been successfully used as effective anticancer drugs in the clinical treatment of cancer. These derivatives are being used for more than 50% of treatment regimes worldwide for cancer patients.[1–3] However, their remarkable success is marred by clinical limitations, including acquired or intrinsic resistance problems, limited spectrum of activity, less target specificity and high toxicity leading to side effects. These limitations have stimulated us to design and synthesize new metal-based drugs with more effectiveness, less toxicity, target specificity and preferably non-covalent DNA binding.[4,5] DNA is the primary intracellular target for anticancer drug design and remains one of the most promising biological receptors for the development of chemotherapeutic agents.[6,7] The interaction between the small molecules of metal-based drugs and DNA can cause DNA damage in cancer cells, consequently blocking the division of cancer cells and resulting in cell death. It is commonly known that metal complexes can interact with DNA non-covalently through electrostatic interactions, groove binding and intercalation.[8] Among these non-covalent binding modes, the intercalation mode attracts considerable attention due to its strong binding ability and various applications in cancer therapy and molecular biology.[9] The intercalating

ability of a molecule with DNA is determined by numerous factors, for example coordination geometry, metal ion size and nature of the ligand.

Furthermore, proteins are also considered to be one of the main molecular targets in the action of anticancer agents. Serum albumins are most extensively studied because of their efficient role in drug delivery and remarkable binding properties with metal complexes.[10,11] Proteins play an important role in the transport and deposition of a variety of endogenous and exogenous substances in blood. The interactions of drugs with them result in the formation of stable drug–protein complexes, which can exert an important effect on the distribution, free concentration and metabolism of a drug in the bloodstream, etc. The binding affinity of drug to serum albumin is pivotal in the design of new drugs.[12,13] Studies of the binding of drugs to albumins are of great importance for obtaining information on structural features that determine the therapeutic effect of drugs. In this regard, bovine serum albumin (BSA) has been extensively studied, due to its structural homology with human serum albumin. Also, some metal ions present in blood plasma affect the binding between drugs and serum albumins and could participate in many biochemical processes. Therefore, knowledge of the reactivity of metal complexes towards DNA and protein BSA is useful for the design and synthesis of metal-based anticancer therapeutics.

Because of the similar coordination modes and chemical properties of palladium(II) and platinum(II), they both form square planar complexes. On the basis of the structural and thermodynamic analogy between platinum(II) and palladium(II) complexes, much attention has been paid to palladium(II) compounds as potential anticancer agents.[14] Palladium(II) complexes undergo aquation and ligand exchange reactions 10^5 times faster than the corresponding platinum(II) complexes.[15] Furthermore, a number of mixed-ligand palladium(II) complexes have been tested and proved to be efficient compounds of antitumor drugs.[16–22] In addition, hydrazones are an important class of ligands with interesting ligation properties due to the presence of several coordination sites and are widely applied in the field of insecticides, medicines and analytical reagents due to their excellent bioactivity.[23,24] The formation of palladium complexes with hydrazone ligand plays an important role in enhancing their biological activity. Herein, we present an investigation of the synthesis, structure, DNA interaction, protein binding, anti-oxidative activity and cytotoxicity of mononuclear palladium complexes of 4-hydroxybenzoic acid (3-ethoxy-2-hydroxybenzylidene)hydrazide. The crystal structures of the new palladium(II) complexes were determined using X-ray crystallography. Biological properties of the prepared complexes (binding properties with calf thymus DNA and competitive binding studies with ethidium bromide) were investigated. The protein binding, cytotoxicity and radical scavenging were also investigated to understand the biological efficacy of the new palladium(II) complexes.

2 | EXPERIMENTAL

2.1 | Materials and physical measurements

Reagent-grade chemicals $PdCl_2{\cdot}2H_2O$, triphenylphosphine, triphenylarsine, 3-ethoxysalicylaldehyde and 4-hydroxybenzoic acid hydrazide were purchased from Sigma-Aldrich and used as received. Calf-thymus DNA (CT-DNA) was purchased from Bangalore Genei, Bangalore, India. BSA was purchased from Himedia Company. All the other chemicals and reagents used for DNA binding, protein binding, antioxidant and cytotoxicity assays were of high quality. Microanalyses (C, H and N) were performed with a Vario EL III CHNS analyser. Infrared (IR) spectra were recorded as KBr pellets in the range 400–4000 cm^{-1} using a PerkinElmer FT-IR 8000 spectrophotometer. Electronic spectra were recorded in dimethylsulfoxide (DMSO) solution with a Systronics 2202 double-beam UV–visible spectrophotometer in the range 200–800 nm. Fluorescence spectral data were acquired with a JASCO FP-8200 fluorescence spectrophotometer at room temperature. ^{1}H NMR, ^{13}C NMR and ^{31}P NMR spectra were recorded with a Bruker AV III 500 MHz instrument using tetramethylsilane and orthophosphoric acid as internal standards. Melting points were recorded with a Veego VMP-DS heating table.

2.2 | Synthesis of hydrazone ligand (H_2L) (1)

The hydrazone ligand 4-hydroxybenzoic acid (3-ethoxy-2-hydroxybenzylidene)hydrazide (**1**) was prepared by refluxing an equimolar mixture of 3-ethoxysalicylaldehde (0.166 g; 1 mM) with 4-hydroxybenzoic acid hydrazide (0.152 g; 1 mM) in 50 ml of methanol for 6 h, as shown in Scheme 1. The reaction mixture was then cooled to room temperature and the solid obtained was filtered, washed several times with distilled water and recrystallized from methanol to afford the ligand in pure form in good yield.

Yield 84%; m.p. 175°C. Anal. Calcd for $C_{16}H_{16}N_2O_4$ (%): C, 63.99; H, 5.37; N, 9.33. Found (%): C, 62.81; H, 5.48; N, 9.10. IR (KBr, cm^{-1}): 3370 ν(NH); 1640 ν(C═O); 1612 ν(C═N). UV–visible (DMSO, λ_{max}, nm): 304, 358 ($\pi \rightarrow \pi^*$, $n \rightarrow \pi^*$). ^{1}H NMR (DMSO-d_6, δ, ppm): 11.91 (s, 1H, hydrazine NH), 8.61 (s, 1H, H─C═N), 11.17 (s, 1H, o-OH), 10.20 (s, 1H, p-OH), 4.02 (q, OCH_2), 1.35 (t, CH_3), 6.81–7.84 (m, 7H, aromatic), 8.47 (s, H─C═N), 9.93 (s, OH), 3.77 (q, O-CH_2), 1.04 (t, CH_3), 6.61–7.95 (m, aromatic). ^{13}C NMR (δ, ppm): 162 (C═O), 160 (C═N), 64 (O─CH_2), 14 (CH_3), 115–147 (aromatic).

2.3 | Synthesis of palladium precursor complexes

The starting complexes $[PdCl_2(PPh_3)_2]$ and $[PdCl_2(AsPh_3)_2]$ were prepared according to previous reports.[25,26]

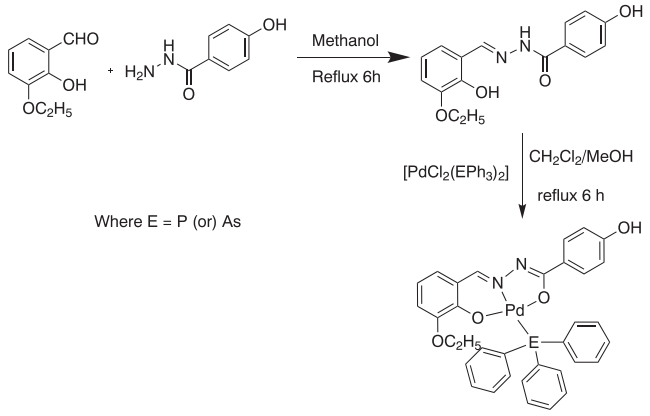

SCHEME 1 Synthesis of ligand and palladium(II) complexes.

2.4 | Synthesis of new palladium(II) hydrazone complexes [Pd(PPh$_3$)L] (**2**) and [Pd(AsPh$_3$)L] (**3**)

Complex **2** was prepared by refluxing equimolar quantities of $[PdCl_2(PPh_3)_2]$ (0.7019 g; 1 mM) in 20 ml of dichloromethane and the hydrazone ligand H_2L (0.3000 g; 1 mM) in 20 ml of methanol (Scheme 1). After a few minutes of mixing the above reactants, two drops of triethylamine were added and continuously refluxed for 6 h. The reaction mixture was then cooled to room temperature, and the resulting product was filtered off, washed with methanol and dried under vacuum. Slow evaporation of **2** from a MeOH–$CHCl_3$ mixture afforded single crystals suitable for X-ray diffraction studies.

Complex **2** ($C_{34}H_{29}N_2O_4PPd$). Yield 81%; m.p. 182°C. Anal. Calcd (%): C, 61.22; H, 4.38; N, 4.20; Found (%): C, 61.65; H, 4.23; N, 4.42. Selected IR bands (cm^{-1}): 1596 ν(C═N); 1350 ν(enolic C─O); 1425, 1033, 691 (for PPh_3). UV–visible (DMSO, λ_{max}, nm): 302, 368 (intraligand transitions); 409, 424 (ligand-to-metal charge transfer). ^{1}H NMR (DMSO-d_6, δ, ppm): 8.51 (s, 1H, H─C═N), 9.89 (s, 1H, p-OH), 3.71 (q, OCH_2), 1.00 (t, CH_3), 6.59–7.77 (m, 22H, aromatic). ^{13}C NMR (δ, ppm): 159 (C─O), 172 (C═N), 64 (O─CH_2), 14 (CH_3), 114–152 (aromatic). ^{31}P NMR (δ, ppm): 17.29.

Complex **3** was synthesised as described above for **2** by utilizing $[PdCl_2(AsPh_3)_2]$ (0.7918 g; 1 mM) and the hydrazone ligand H_2L (0.3000 g; 1 mM) as in Scheme 1. Slow evaporation of **3** from a MeOH–$CHCl_3$ mixture afforded single crystals suitable for X-ray diffraction studies.

Complex **3** ($C_{34}H_{29}N_2O_4AsPd$). Yield 78%; m.p. 191°C. Anal. Calcd (%): C, 57.44; H, 4.11; N, 3.94. Found (%): C, 56.73; H, 4.32; N, 4.06. Selected IR bands (cm^{-1}): 1598 ν(C═N); 1357 ν(enolic C─O); 1435, 1080, 693 (for $AsPh_3$). UV–visible (DMSO, λ_{max}, nm): 305, 368 (intraligand transitions); 406, 432 (ligand-to-metal charge transfer). ^{1}H NMR (DMSO-d_6, δ, ppm): 8.57 (s, 1H, H─C═N), 9.93 (s, 1H, p-OH), 3.77 (q, OCH_2), 1.04 (t, CH_3), 6.61–7.95 (m, 22H, aromatic). ^{13}C NMR (δ, ppm): 159 (C─O), 172 (C═N), 63 (O─CH_2), 14 (CH_3), 115–152 (aromatic).

2.5 | Crystal structure determination

Single-crystal X-ray diffraction data of **2** and **3** were collected at room temperature with a Bruker AXS KAPPA APEX2 CCD diffractometer equipped with a fine focused sealed tube. The unit cell parameters were determined and the data collections of **2** and **3** were performed using graphite-monochromated Mo Kα radiation (k = 0.71073 Å) by u and x scans. The data collected were reduced using the SAINT program[27] and the empirical absorption corrections were carried out using the SADABS program.[28] The structure of the ligand and complexes was solved by direct methods[29] using SHELXS-97, which revealed the position of all non-hydrogen atoms, and was refined by full-matrix least squares on F^2 (SHELXL-97).[30] All non-hydrogen atoms were refined anisotropically, while the hydrogen atoms were placed in calculated positions and refined as riding atoms.

2.6 | DNA binding studies

Experiments involving the interaction of the free hydrazone ligand and its palladium(II) complexes with DNA were carried out in double-distilled water containing tris (hydroxymethyl)aminomethane buffer (Tris; 5 mM) and NaCl (50 mM) and the pH was adjusted to 7.2 with hydrochloric acid. Stock solution of CT-DNA was stored at 277 K and used only for a period of four days. The concentration of CT-DNA was determined by UV absorbance at 260 nm and its molar absorption coefficient was taken as 6600 M^{-1} cm^{-1}.[31] Solutions of CT-DNA in Tris–HCl buffer gave a ratio of UV absorbance at 260 and 280 nm of approximately 1.8–1.9, indicating that the DNA was sufficiently free of protein. Concentrated stock solutions of ligand **1** and palladium(II) complexes **2** and **3** were prepared in DMSO and diluted with Tris–HCl buffer to required concentrations. Absorption spectral titration was performed by keeping the concentration of the test compounds constant while varying the CT-DNA concentration. Equal volume of CT-DNA solution was added to the reference solution to eliminate the absorbance of CT-DNA itself.

Competitive studies of each compound with ethidium bromide (EB) were conducted with fluorescence spectroscopy in order to examine whether the compound can displace EB from the DNA–EB complex. The DNA–EB complex was prepared by adding 10 μM EB and CT-DNA in buffer. The binding effect of ligand and complexes with the DNA–EB complex was studied by adding a certain amount of a solution of the test compound step by step into a solution of the DNA–EB complex. The influence of the addition of each compound to the DNA–EB complex solution was determined by recording the variation of fluorescence emission spectra. Electrochemical titration experiments were performed by keeping the concentration of the test compounds constant while varying the CT-DNA concentration using Tris–HCl buffer as electrolyte. The relative viscosities for DNA in the absence

(η_0) and presence (η) of the compounds was calculated using the relation $\eta = (t - t_0)/t_0$, where t and t_0 are the observed flow time for each sample and buffer. The values of relative viscosity $(\eta/\eta_0)^{1/3}$ were plotted against R, where R = [DNA]/[compound].

2.7 | BSA binding studies

The protein binding study was performed by tryptophan fluorescence quenching experiments using BSA. The excitation wavelength of BSA at 280 nm and the quenching of the emission intensity of tryptophan residues of BSA at 345 nm were monitored using the complexes as quenchers with increasing concentrations.[32] The excitation and emission slit widths and scan rates were kept constant for all experiments. A stock solution of BSA was prepared using 50 mM NaCl/Tris–HCl (pH = 7.2) and stored in the dark at 4°C for further use. Concentrated stock solutions of ligand and complexes were prepared by dissolving them in DMSO/Tris–HCl buffer (1:100) and diluted suitably with buffer to required concentrations. An amount of 2.5 ml of BSA solution (1 μM) was titrated by successive additions of a 25 ml stock solution of compounds (0–25 μM) using a micropipette.

2.8 | Antioxidant assays

The 2,2-diphenyl-1-picrylhydrazyl (DPPH) radical scavenging activity of the synthesized compounds was measured according to the method of Blois.[33] The DPPH radical is a stable free radical having λ_{max} at 517 nm. A fixed concentration of the experimental compounds was added to a solution of DPPH in methanol (125 μM, 2 ml), and the final volume was made up to 4 ml with double-distilled water. The solution was incubated at 37°C for 30 min in the dark. The decrease in absorbance of DPPH was measured at 517 nm.

The hydroxyl radical scavenging activities of the compounds were investigated using the Nash method.[34] *In vitro* hydroxyl radicals were generated by Fe^{3+}/ascorbic acid system. The detection of hydroxyl radicals was carried out by measuring the amount of formaldehyde formed from the oxidation reaction with DMSO. The formaldehyde produced was detected spectrophotometrically at 412 nm. A mixture of 1.0 ml of iron–EDTA solution (0.13% ferrous ammonium sulfate and 0.26% EDTA), 0.5 ml of EDTA solution (0.018%) and 1.0 ml of DMSO (0.85% DMSO (*v*/v) in 0.1 M phosphate buffer, pH = 7.4) were sequentially added in the test tubes. The reaction was initiated by adding 0.5 ml of ascorbic acid (0.22%) and incubated at 80–90°C for 15 min in a water bath. After incubation, the reaction was terminated by the addition of 1.0 ml of ice-cold trichloroacetic acid (17.5% *w*/*v*). Subsequently, 3.0 ml of Nash reagent was added to each tube and left at room temperature for 15 min. The intensity of the colour formed was measured spectrophotometrically at 412 nm against a reagent blank.

Assay of nitric oxide scavenging activity was based on the Green method,[35] where sodium nitroprusside in aqueous solution at physiological pH spontaneously generates nitric oxide, which interacts with oxygen to produce nitrite ions that can be estimated using Greiss reagent. Scavengers of nitric oxide compete with oxygen leading to reduced production of nitrite ions. For the experiment, sodium nitroprusside (10 mM) in phosphate-buffered saline (PBS) was mixed with a fixed concentration of the test compound and incubated at room temperature for 150 min. After the incubation period, 0.5 ml of Griess reagent containing 1% sulfanilamide, 2% H_3PO_4 and 0.1% *N*-(1-naphthyl)ethylenediamine dihydrochloride was added. The absorbance of the chromophore formed was measured at 546 nm.

For each of the above assays, tests were done in triplicate by varying the concentration of the complexes ranging from 10 to 50 μM. The percentage activity was calculated by using the following formula: activity (%) = $[(A_0 - A_c)/A_0] \times 100$, where A_0 and A_c represent the absorbance in the absence and presence of the test compounds, respectively. The 50% activities (IC_{50}) were calculated from the results of percentage activity.

2.9 | Cytotoxicity studies

Cytotoxicity of the ligand and palladium(II) complexes was evaluated against human cervical (HeLa) and human breast (MCF-7) cell lines. Cell viability was determined using the 3-(4,5-dimethylthiazol-2-yl)-2,5-diphenyltetrazolium bromide (MTT) assay method.[36] The MCF-7 and HeLa cells were grown in Eagle's minimum essential medium containing 10% foetal bovine serum. For screening experiment, the cells were seeded into 96-well plates in 100 ml of respective medium. The test compounds (**1**–**3**) dissolved in DMSO were seeded to the wells. Triplication was maintained, and the medium without the compounds served as the control. After 24 h, the wells were treated with 20 μl of MTT (5 mg ml^{-1} PBS) and incubated at 37°C for 4 h. The medium with MTT was then removed separately and the formed formazan crystals were dissolved in 100 ml of DMSO. The absorbance was then measured at 570 nm using a microplate reader. The percentage cell inhibition was determined using the following equation: cell inhibition (%) = 100 − Abs(sample)/Abs(control) × 100. The IC_{50} values were determined from a graph of percentage cell inhibition plotted against concentration.

3 | RESULTS AND DISCUSSION

3.1 | Synthesis of complexes

The reaction of H_2L with $[PdCl_2(PPh_3)_2]$ and $[PdCl_2(AsPh_3)_2]$ (1:1) affords new complexes $[Pd(PPh_3)L]$ (**2**) and $[Pd(AsPh_3)L]$ (**3**) (Scheme 1). It is found that the ligand coordinates in a dibasic tridentate nature. All the synthesized compounds were characterized using elemental analysis and IR,

UV–visible, ^{1}H NMR, ^{13}C NMR and ^{31}P NMR spectroscopies; data are given in Section 2. The structures of **2** and **3** were confirmed from the X-ray crystallographic study.

3.2 | Spectroscopic studies

The characteristic IR bands of the new palladium(II) complexes were compared with those of the free ligand (H_2L) and provide significant information regarding the coordination mode of ligand in metal complexes. The spectrum of the free ligand displays a peak at 1640 cm^{-1} for C═O and it is absent in the spectra of the complexes. This observation may be attributed to the enolization of ─NH─C═O and subsequent coordination through the deprotonated oxygen.[37] The bands observed at 1350 and 1357 cm^{-1} (**2** and **3**) due to C─O further confirm the coordination through the deprotonated oxygen. The ligand shows a strong band at 1612 cm^{-1} which is characteristic of the azomethine group (>C═N). Coordination of the ligand to the palladium ion through azomethine nitrogen atom is expected to reduce the electron density in the azomethine link and thus lowers the C═N band frequency in the region 1596 and 1598 cm^{-1}.[38,39] The spectrum of the ligand shows a medium to strong band at around 3370 cm^{-1} which is characteristic of N─H functional group. This band disappeared in the spectra of the complexes due to deprotonation of phenolic oxygen prior to coordination to the palladium(II) ion. In addition, the palladium(II) hydrazone complexes show strong vibrations is the expected region confirming the presence of triphenylphosphine and arsine.[40] The electronic spectra of ligand and complexes show two to four bands in the region 302–432 nm. The bands appearing in the region 302–368 nm are assigned to intraligand transition[41] and the bands around 406–432 nm are assigned to metal-to-ligand charge transfer transition.[42]

The ^{1}H NMR spectra of all the synthesized compounds were recorded in DMSO-d_6 to confirm the binding of the benzoylhydrazone ligand to the palladium(II) ion. The free ligand shows a broad signal at 11.17 ppm due to *ortho*-OH group. In the spectra of complexes, the signal of the phenolic proton is absent due to deprotonation. However, ligand and complexes demonstrate a singlet at 9.93–10.20 ppm which indicates the non-participation of *para*-OH from coordination. The NMR spectrum of the ligand shows a singlet at 11.91 ppm corresponding to ─NH group. Interestingly, in the spectra of the complexes, there is no resonance attributable to ─NH, indicating the coordination of ligand in the anionic form upon deprotonation.[43] A sharp singlet at 8.61 ppm is due to the azomethine proton. The positions of the azomethine signal in the spectra of the complexes are slightly upfield when compared with those of the free ligand, suggesting that the azomethine proton is coordinated to palladium ion. In the spectra of ligand and complexes, the multiplet observed at around 6.59–7.95 ppm is assigned to aromatic protons of the phenyl group of triphenylphosphine/triphenylarsine. The results confirm the coordination mode of benzoylhydrazone ligand to palladium(II) ion via the phenolate oxygen, the azomethine nitrogen and imidolate oxygen and also the presence of PPh_3/$AsPh_3$ groups.

The ^{13}C NMR spectrum of the ligand demonstrates a signal at 162 ppm corresponding to the carbonyl carbon (C═O), which disappears for the complexes and a new signal at 159 ppm (C─O) is observed, which indicates the coordination of oxygen via deprotonation. The ligand displays a single resonance at 160 ppm due to the azomethine carbon atom. The downfield shift of this signal for the complexes at 172 ppm clearly indicates the coordination of the azomethaine group. The aromatic carbons of the free ligand and complexes show signals in the region 114–152 ppm. The signals due to CH_2 and CH_3 carbons of ligand and complexes appear at 64 and 14 ppm, respectively.

In order to confirm the presence of triphenylphosphine group, the ^{31}P NMR spectrum was recorded for complex **2**. A sharp singlet is observed at 17.29 ppm which shows the presence of phosphorous atom and thus suggesting the presence of triphenylphosphine group in complex **2**.[44]

3.3 | X-ray crystallography

The molecular structures of complexes **2** and **3** were determined using single-crystal X-ray diffraction to find out the coordination mode of the hydrazone ligand in the complexes and stereochemistry of the complexes. The ORTEP views of complexes **2** and **3** are shown in Figures 1 and 2, respectively. A summary of data collection and refinement parameters is given in Table 1, whereas selected bond lengths and bond angles are given in Table 2. Complex **2** crystallizes in triclinic space group P1 whereas the complex **3** crystallizes in monoclinic space group $P2_1/c$. The hydrazone ligand coordinates with the metal at O, N and O forming one five-membered and one six-membered chelate ring with bite angles of 79.72(7)° N(28)–Pd(1)–O(31) and 93.97(7)° N(28)–Pd(1)–O(35) and bond lengths of 1.9744(18) Å Pd(1)–N(28),

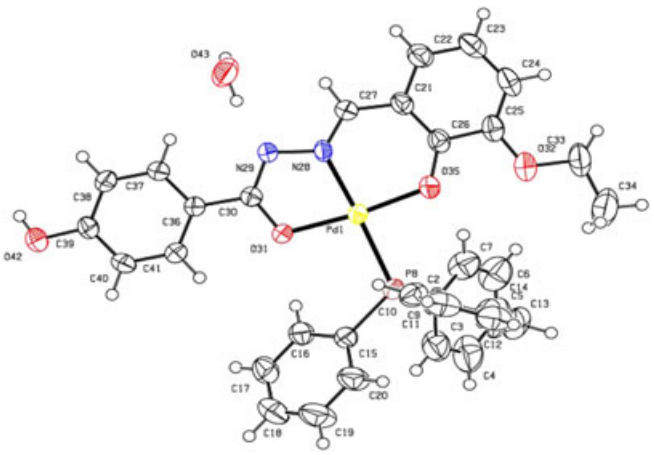

FIGURE 1 ORTEP diagram of **2** with thermal ellipsoids at 50% probability.

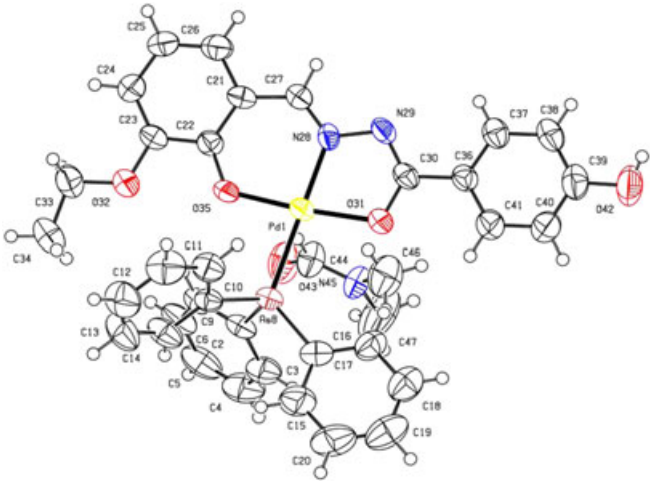

FIGURE 2 ORTEP diagram of **3** with thermal ellipsoids at 50% probability.

1.9867(16) Å Pd(1)–O(31) and 1.9684(16) Å Pd(1)–O(35) for complex **2**, and bite angles of 79.79(13)° N(28)–Pd(1)–O(31) and 95.06(13)° N(28)–Pd(1)–O(35) and bond lengths of 1.971(4) Å Pd(1)–N(28), 1.993(3) Å Pd(1)–O(31) and 1.963(3) Å Pd(1)–O(35) for complex **3**. The remaining binding site is occupied by the triphenylphosphine unit Pd(1)–P(8) bond distance of 2.2888(6) Å and triphenylarsine unit Pd(1)–As(8) bond distance 2.3920(5) Å for **2** and **3**, respectively. The bond angles O(31)–Pd(1)–O(35) 173.62(6)°, N(28)–Pd(1)–P(8) 176.67(5)° for complex **2**, and O(31)–Pd(1)–O(35) 174.63(13)°, N(28)–Pd(1)–As(8) 179.51(10)° for complex **3** deviate considerably from the ideal angle of 180° causing significant distortion in the square planar geometry of the complexes. The selected bond lengths and bond angles agree very well with those reported for other palladium(II) complexes.[45]

3.4 | DNA binding studies

3.4.1 | Electronic absorption titration

Both covalent and non-covalent interactions are involved between transition metal complexes and DNA. In the case of covalent binding, the labile ligands of complexes is replaced by a nitrogen base of DNA such as guanine N7 while the non-covalent DNA interactions include intercalative, electrostatic and groove binding of metal

TABLE 1 Crystal and structure refinement data

	2	**3**
Empirical formula	$C_{34}H_{31}N_2O_5PPd$	$C_{37}H_{36}AsN_3O_5Pd$
Formula weight	685.02	784.01
Temperature (K)	295.3(3)	296
Wavelength (Å)	0.71073	0.71073
Crystal system	Triclinic	Monoclinic
Space group	P1	$P2_1/c$
Unit cell dimensions		
a (Å)	9.6660(4)	11.5575(11)
b (Å)	12.3195(5)	26.1997(17)
c (Å)	13.3136(6)	11.6320(7)
α (°)	103.326(4)	90
β (°)	91.705(4)	98.039(6)
γ (°)	90.266(3)	90
Volume (Å^3)	1541.91(12)	3487.6(5)
Z	2	4
Density (calculated) (Mg m^{-3})	1.4754	1.4988
Absorption coefficient (mm^{-1})	0.698	1.522
F(000)	698.5	1588.9
Crystal size (mm^3)	0.23 × 0.23 × 0.21	0.69 × 0.59 × 0.56
θ range for data collection (°)	6.56 to 57.48	6.22 to 57.5
Index ranges	$-13 \le h \le 12$, $-15 \le k \le 15$, $-17 \le l \le 16$	$-14 \le h \le 12$, $-31 \le k \le 32$, $-15 \le l \le 15$
Reflections collected	12 172	10 998
Independent reflections	6969 [R(int) = 0.0195]	6670[R(int) = 0.0336] = 0.0336]
Refinement method	Full-matrix least-squares on F^2	Full-matrix least-squares on F^2
Data/restraints/parameters	6969/0/392	6670/0/427
Goodness-of-fit on F^2	1.068	1.080
Final R indices [$I > 2\sigma(I)$]	$R_1 = 0.0311$, $wR_2 = 0.0851$	$R_1 = 0.0495$, $wR_2 = 0.0456$
R indices (all data)	$R_1 = 0.0394$, $wR_2 = 0.0780$	$R_1 = 0.0796$, $wR_2 = 0.1123$
Largest diff. Peak and hole (e Å^{-3})	0.52 and −0.64	1.02 and −0.80

TABLE 2 Selected bond lengths (Å) and angles (°) of complexes **2** and **3**

2		3	
Bond lengths			
Pd(1)–N(28)	1.9744(18)	Pd(1)–N(28)	1.971(4)
Pd(1)–O(31)	1.9867(16)	Pd(1)–O(31)	1.993(3)
Pd(1)–O(35)	1.9684(16)	Pd(1)–O(35)	1.963(3)
Pd(1)–P(8)	2.2888(6)	Pd(1)–As(8)	2.392(5)
N(28)–N(29)	1.395(2)	N(28)–N(29)	1.379(5)
N(28)–C(27)	1.281(3)	N(28)–C(27)	1.273(5)
O(35)–C(26)	1.319(3)	O(35)–C(22)	1.307(5)
O(31)–C(30)	1.298(3)	O(31)–C(30)	1.317(5)
N(29)–C(30)	1.301(3)	N(29)–C(30)	1.300(6)
Bond angles			
O(31)–Pd(1)–O(35)	173.62(6)	O(31)–Pd(1)–O(35)	174.63(13)
N(28)–Pd(1)–P(8)	176.67(5)	N(28)–Pd(1)–As(8)	179.51(10)
N(28)–Pd(1)–O(35)	93.97(7)	N(28)–Pd(1)–O(31)	79.79(13)
N(28)–Pd(1–O(31)	79.72(7)	N(28)–Pd(1)–O(35)	95.06(13)

complexes outside of the DNA helix. An absorption titration experiment was carried out to study the DNA binding properties of the new synthesized compounds (**1**–**3**). The absorption spectra of the compounds at a constant concentration (25 μM) in the presence of various concentrations of CT-DNA (10–50 μM) are shown in Figure 3. Upon incremental additions of DNA to the ligand solution, the absorption bands of H_2L observed at 228 and 309 nm exhibit a hypochromism of about 31 and 5% without any shift in the band positions. This reveals that there is an interaction between the ligand and DNA through intercalation or some other mode of binding. However, complex **2** exhibits a hypochromism of about 30, 18 and 14% with a hypsochromic shift of 3, 2 and 2 nm at 267, 330 and 404 nm. Similarly, absorption bands of complex **3** found at 267, 329 and 403 nm exhibit the same phenomenon of hypochromism of about 33, 32 and 23%, respectively, with a hypsochromic shift of about 2 nm. These results suggest an intimate association of complexes **2** and **3** with CT-DNA, and it is also likely that they bind to the DNA helix via intercalation.[46] After the compounds intercalate to the base pairs of DNA, the π* orbital of the intercalated compounds could couple with π orbitals of the base pairs, thus decreasing the π → π* transition energies, resulting in hypochromism. Complexes **2** and **3** show more hypochromicity with red shift than the ligand, indicating that the binding strength of the palladium(II) complexes is much stronger than that of the free ligand. The magnitude of the binding strength of the compounds with CT-DNA can be estimated through the binding constant K_b, which can be obtained by monitoring the changes in the absorbance of the corresponding λ_{max} with increasing concentrations of CT-DNA and is given by

$$\frac{[DNA]}{\varepsilon_a - \varepsilon_f} = \frac{[DNA]}{\varepsilon_b - \varepsilon_f} + \frac{1}{K_b(\varepsilon_b - \varepsilon_f)}$$

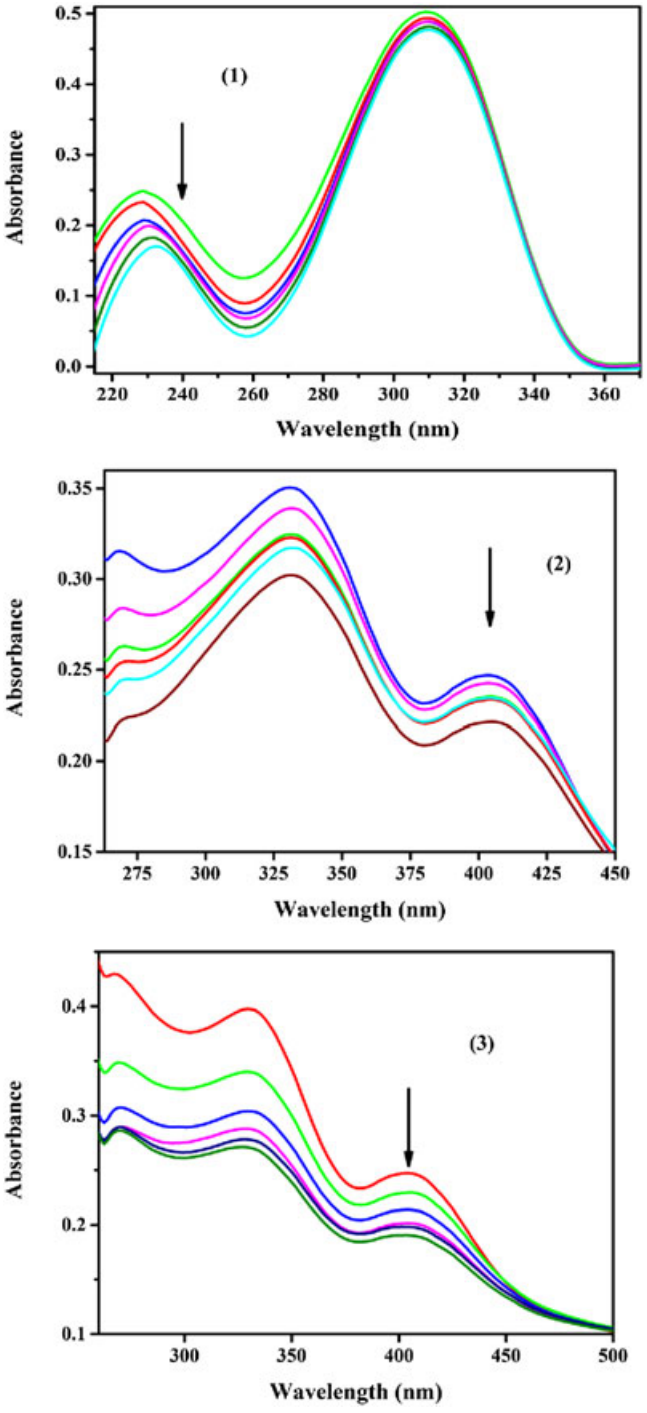

FIGURE 3 Electronic spectra of compounds **1**, **2** and **3** in Tris–HCl buffer upon addition of CT-DNA. [Compound] = 25 μM, [DNA] = 0–50 μM. Arrows show that the absorption intensities decrease with increasing DNA concentration.

Where [DNA] is the concentration of DNA in base pairs, ε_a is the extinction coefficient observed at a given DNA concentration, ε_f is the extinction coefficient of the free complex in solution and ε_b is the extinction coefficient of the complex when fully bound to DNA. In plots of [DNA]/($\varepsilon_a - \varepsilon_f$) versus [DNA], K_b is given by the ratio of slope to intercept.

The magnitudes of the intrinsic binding constants (K_b) were calculated to be 1.42×10^4 M^{-1} for the H_2L),

7.09×10^4 M^{-1} for complex **2** and 3.71×10^4 M^{-1} for complex **3** (Figure 4 and Table 3). The observed values of K_b reveal that the ligand and palladium(II) complexes bind to DNA via an intercalative mode. These results are similar to previously reported values for the intercalative mode of various metallointercalators.[47,48] The larger aromatic moiety in complexes **2** and **3** facilitates its potential intercalative DNA binding. Based on the K_b value, we can arrange the compounds in the following order: **2** > **3** > **1**.

3.4.2 | EB displacement study

The binding of compounds **1**–**3** to CT-DNA was studied by evaluating the fluorescence emission intensity of EB bound to DNA (EB–DNA) upon the addition of the compounds. EB is one of the most sensitive fluorescence probes that can bind with DNA. The fluorescence of EB increases after intercalating into DNA. If a metal complex intercalates into DNA, it leads to a decrease in the binding sites of DNA available for EB, resulting in decrease in the fluorescence intensity of the CT-DNA–EB system. The extent of decrease in the fluorescence intensity (quenching) of CT-DNA–EB reflects the extent of interaction of the complex with CT-DNA. Figure 5 shows the fluorescence spectra of EB–DNA with increasing amounts of the test compounds. As the concentration of the compounds increases, the emission band at 613 nm exhibits hypochromism up to 60, 84 and 68% with blue shifts of 2 nm of the initial fluorescence intensity for **1**, **2** and **3**, respectively. The EB–DNA quenching results also indicate that many of the EB molecules have been displaced from the EB–DNA complex by each quencher at the approximate titration end point and that the intercalation takes place between the test compounds and DNA. Comparatively, free ligand can compete with EB in binding to DNA and complex **2** binds to DNA stronger than **1** and **3**.

The quenching data were analysed according to the Stern–Volmer equation, and the K_q value is obtained as the

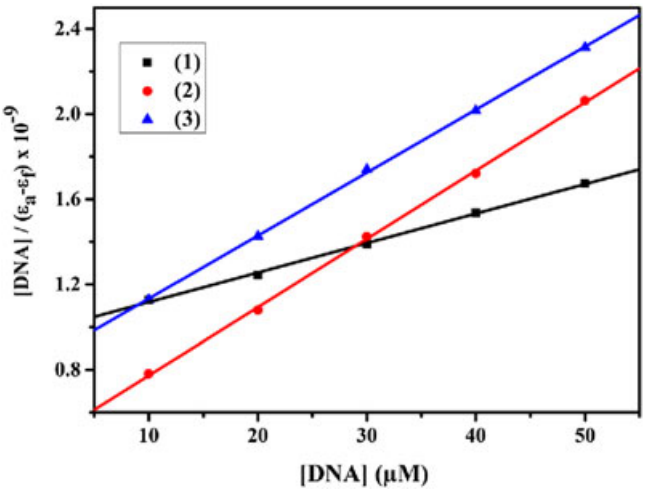

FIGURE 4 Plots of [DNA]/($\varepsilon_a - \varepsilon_f$) versus [DNA] for compounds **1**–**3** with CT-DNA.

TABLE 3 DNA binding constants (K_b), quenching constants (K_q) and apparent binding constants (K_{app})

Compound	K_b (M^{-1})	K_q (M^{-1})	K_{app} (M^{-1})
1	1.42×10^4	2.53×10^4	1.8×10^5
2	7.09×10^4	1.07×10^5	8.1×10^5
3	3.71×10^4	2.82×10^4	3.1×10^5

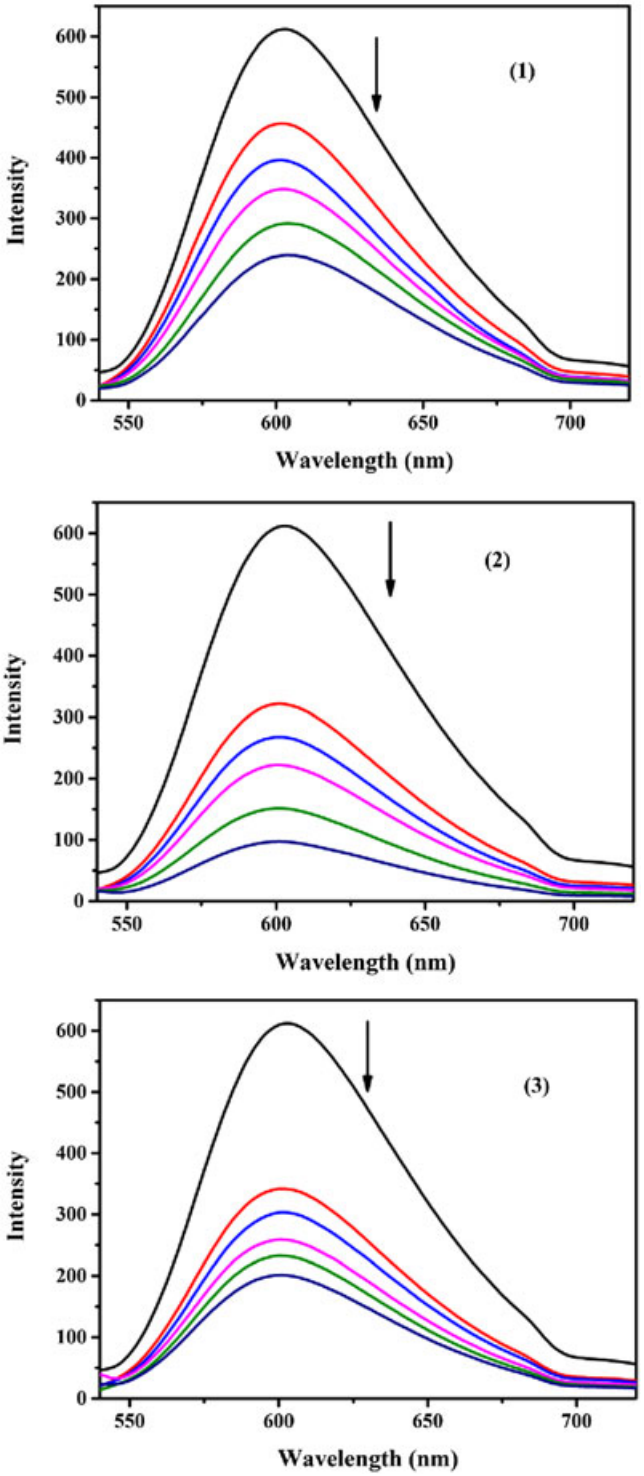

FIGURE 5 Fluorescence quenching curves of EB bound to DNA for **1**, **2** and **3**. [DNA] = 10 μM, [EB] = 10 μM, [complex] = 0–50 μM. Arrows show the emission intensity changes with increasing complex concentration.

slope of a plot of I_0/I versus [Q]. The quenching plots illustrate that the quenching of EB bound to CT-DNA by the complexes are in good agreement with the linear Stern–Volmer equation. The K_q values for the compounds are given in Table 3. Further, the binding constant (K_{app}) value obtained for the compounds using the following equation are given in Table 3:

$$K_{EB}[EB] = K_{app}[compound]$$

where the compound concentration is the value at a 50% reduction in the fluorescence intensity of EB, K_{EB} (1.0×10^7 M^{-1}) is the DNA binding constant of EB and [EB] is 10 μM.

The apparent binding constants are found to be 1.8×10^5, 8.1×10^6 and 3.1×10^5 M^{-1} for **1**, **2** and **3**, respectively (Figure 6). These results suggest that the interaction of the palladium(II) complexes with CT-DNA is stronger than that of the free ligand, which is consistent with the absorption spectral observations. The quenching constants and binding constants of the ligand and Pd(II) complexes suggest that the interaction of all the compounds with DNA should be of an intercalative nature.[49] On the basis of all the spectroscopic studies, we conclude that the free ligand and Pd(II) complexes can bind to CT-DNA via an intercalative mode and also that complexes **2** and **3** bind to CT-DNA more strongly than the free ligand. This result also indicates that compounds **1**–**3** bind strongly to the DNA probably by intercalative interaction which is supported by the absorption titration experiment.

3.4.3 | Cyclic voltammetry

The application of electrochemical methods to the study of interaction of metal complexes to DNA provides a useful complement to other methods, such as UV–visible and fluorescence spectroscopies. In general, the electrochemical potential of a small molecule will shift positively when it intercalates into a DNA double helix, and it will shift in a negative direction in the case of electrostatic interaction with DNA.[50] Upon incremental addition of CT-DNA to a complex solution, new redox peaks do not appear and the current intensity decreases, suggesting the occurrence of interaction between each metal complex and CT-DNA. The decrease in current intensity can be explained in terms of an equilibrium mixture of free and DNA-bound complex at the electrode surface.[51] The cyclic voltammograms of Pd(II) complexes **2** and **3** in the absence and presence of CT-DNA are shown in Figure 7. In the presence of DNA, both the cathodic (E_{pc}) and the anodic (E_{pa}) potentials of **2** and **3** exhibit a positive shift, while the current peaks decrease significantly suggesting the existence of an interaction between each complex and CT-DNA. The above results reveal an intercalative mode of binding between the complexes and CT-DNA base pairs.

3.4.4 | Viscosity experiments

To further confirm the interaction mode of the complexes with DNA, a viscosity study was carried out. The addition of the compounds into DNA solution results in a significant increase of the relative viscosity of DNA; this increase may be explained by an increase of the overall DNA length caused

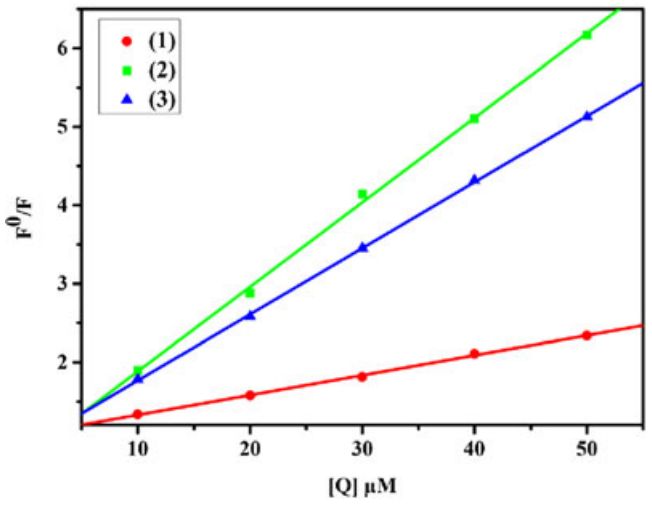

FIGURE 6 Stern–Volmer plots of EB–DNA fluorescence titrations for compounds **1**–**3**.

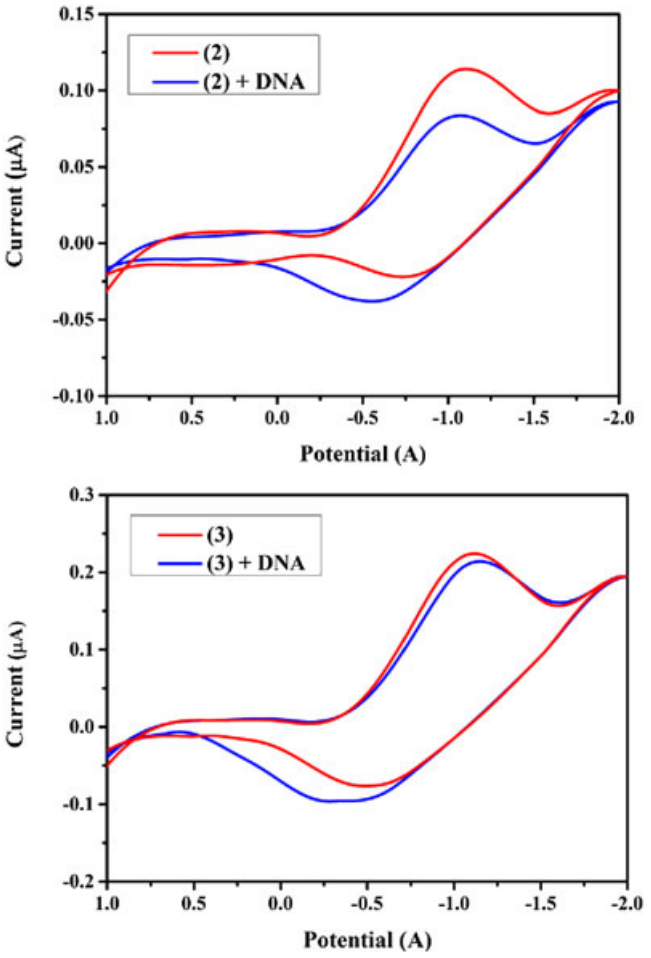

FIGURE 7 Cyclic voltammograms of complexes **2** and **3** in the absence and presence (inner curve) of DNA (10 μM). Scan rate: 100 mV s^{-1}.

by the insertion of the complexes in between the DNA base pairs which increases the separation of base pairs at intercalation sites.[52] The relative viscosity of DNA changes with the amount of compounds (Figure 8). These results suggest that the viscosity of DNA increases on addition of compounds **1**–**3**. In general, the viscosity of DNA increases steadily when compounds intercalate between adjacent DNA base pairs. The increased degree of viscosity, which may depend on affinity to DNA, follows the order **2** > **3** > **1**.

On the basis of the above discussion of DNA binding for the ligand and two complexes, it has been shown, as a result of binding energy, that the complexes have a greater DNA-binding affinity than the free ligand. The positive results of DNA binding studies for the ligand and complexes prompted us to study their protein BSA-binding activity.

3.5 | BSA binding properties

3.5.1 | Fluorescence quenching of BSA by compounds

Proteins are important chemical substances and major targets for many types of medicines. Interaction of metal complexes with proteins is becoming increasingly important for interpreting metabolism and transport processes. In the present work, BSA was chosen as the model protein due to its structural homology with human serum albumin, its availability, low cost and unusual ligand binding properties. BSA contains three fluorophores, i.e. tryptophan, tyrosine and phenylalanine, and the intrinsic fluorescence of BSA is mainly due to tryptophan alone and changes in the emission spectra of tryptophan are common in response to protein conformational transitions, subunit associations, substrate binding or denaturation. Furthermore, the binding of metal complexes to proteins may provide information on the relationship between structures and functions of proteins. Therefore, the binding of the synthesized compounds to BSA can be studied by examining fluorescence spectra.

The binding activities of the ligand and complexes with BSA protein were studied using fluorescence measurements at room temperature. A solution of BSA (1 μM) was titrated with various concentrations of the complexes (0–25 μM). Fluorescence spectra were recorded in the range 290–500 nm upon excitation at 280 nm. The changes observed in the fluorescence emission spectra of a solution of BSA on the addition of increasing amounts of test compounds are shown in Figure 9. As can be seen, the fluorescence emission intensities of BSA at 348 nm show significant decreasing trends with increasing concentration of the test compounds, indicating that the interaction of the

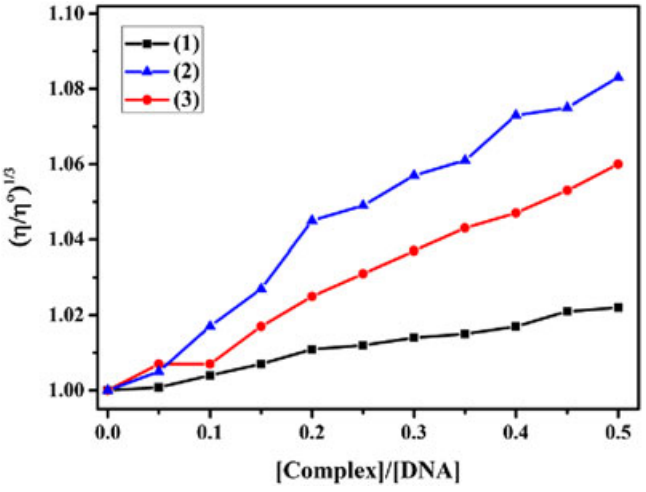

FIGURE 8 Effect of compounds **1**–**3** on viscosity of CT-DNA.

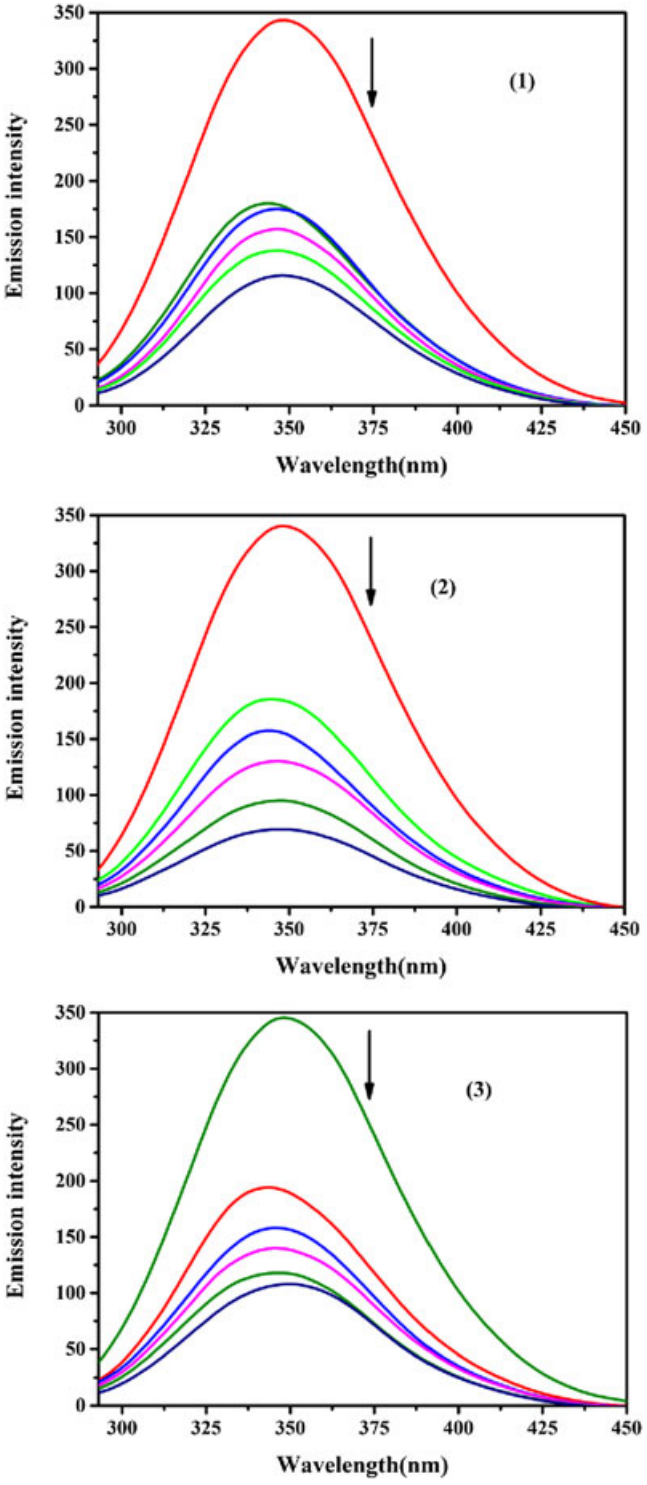

FIGURE 9 Fluorescence titrations of **1**–**3** (0–25 μM) with BSA (1 μM).

compounds with BSA could cause conformational changes in protein structure, leading to changes in the tryptophan microenvironment of BSA. Upon addition of the compounds to the BSA solution, a significant decrease of the fluorescence intensity of BSA at 348 nm up to 66, 79 and 68% of the initial fluorescence intensity of BSA accompanied by a bathochromic shift of 1, 2 and 3 nm for compounds **1**–**3**, respectively, are observed. The observed red shift is mainly due to the binding of compounds with the active site in BSA.[53] These results suggest a definite interaction of all the complexes with the BSA protein.

In addition, the fluorescence quenching data were analysed with the Stern–Volmer equation and the Scatchard equation. From a plot of F_0/F versus [Q], the quenching constant (K_q) can be calculated (Figure 10). It is assumed that the binding of the compounds with BSA occurs at equilibrium and the equilibrium binding constant can be analysed according to the Scatchard equation:

$$\log\left(\frac{F_0-F}{F}\right) = \log K_{bin} + n\log[Q]$$

where K_{bin} is the binding constant of the compound with BSA and n is the number of binding sites. K_{bin} and n have been calculated from plots of log[$(F_0 - F)/F$] versus log[Q] (Figure 11). The calculated K_q, K_{bin} and n values are listed in Table 4. The calculated value of n is around 1 for all of the compounds, indicating the existence of just a single binding site in BSA for all of the compounds. Also, the results show that complex **2** interacts with BSA more strongly than complex **3** and ligand **1**.

3.5.2 | UV absorption spectra of BSA in the presence of compounds

Results of UV absorption spectral titrations of BSA in the presence and absence of ligand and complexes are shown in Figure 12. It is seen that there is a decrease in the absorption

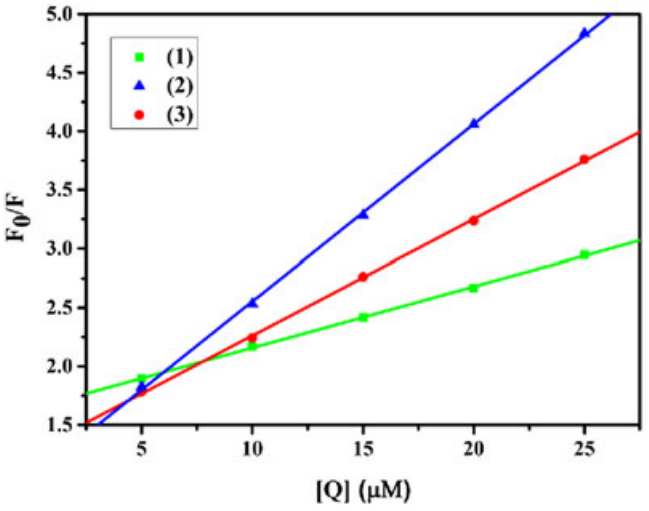

FIGURE 10 Stern–Volmer plots of fluorescence titrations of **1**–**3** with BSA.

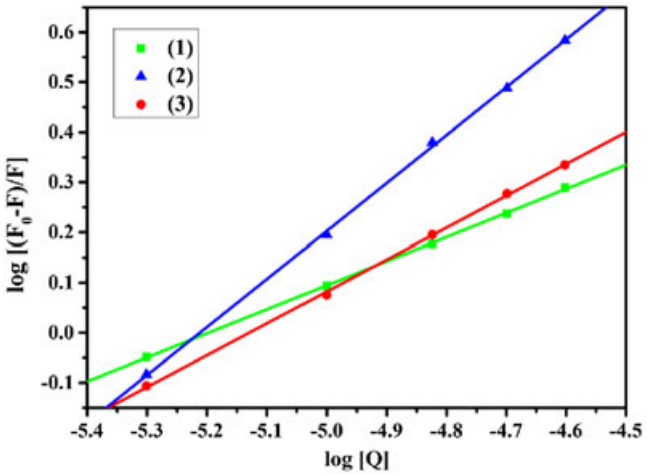

FIGURE 11 Plots of log[Q] versus log[$(F_0 - F)/F$].

TABLE 4 Quenching constants (K_q), binding constants (K_{bin}) and number of binding sites (n) for interactions of compounds **1**–**3** with BSA

Compound	K_q (M^{-1})	K_{bin} (M^{-1})	n
1	5.2×10^4	6.3×10^4	0.89
2	1.5×10^5	8.4×10^5	1.21
3	6.9×10^4	7.0×10^4	0.94

intensity of BSA with the addition of the test compounds and there is a small red shift of about 1 nm for compounds **1**, **2** and **3**. From the results obtained it is concluded that only a static interaction takes place between the tested compounds **1**–**3** and BSA.[54]

3.6 | Antioxidant activity

The antioxidative properties of hydrazone ligand H_2L and its metal complexes have attracted a lot of interest recently and have been extensively investigated, mainly in *in vitro* systems. The antioxidant potential of the new palladium complexes along with that of standard ascorbic acid in cell-free systems has been examined with reference to DPPH radicals, nitric oxide radicals (NO) and hydroxyl radicals (OH) and their corresponding IC_{50} (determination of 50% activity) values are given in Table 5. The IC_{50} values of all test compounds obtained from different types of assay experiments strongly support that the complexes investigated in this work possess excellent antioxidant activities, which are better than that of the standard antioxidant ascorbic acid. The antioxidant activity of the free ligand H_2L is observed to be less effective on the free radicals. The new complexes **2** and **3** having similar structure show significant antioxidant activities. Among the Pd(II) complexes, that containing triphenylphosphine as a co-ligand shows better activities than that containing triphenylarsine. From these results, it is clear that the scavenging effects of the free ligand are significantly less when compared to the corresponding Pd(II) complexes, which is

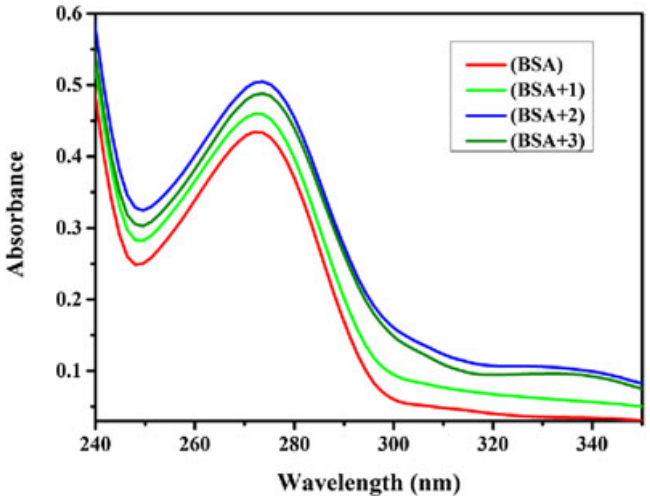

FIGURE 12 Absorption titrations of **1–3** with BSA.

TABLE 5 Antioxidant activity of ligand, complexes and standard ascorbic acid

Compound	IC_{50} (μM)		
	DPPH•	OH•	NO•
1	95.11	90.73	85.92
2	43.01	17.15	58.37
3	52.34	19.45	58.73
Ascorbic acid	27.71	5.12	37.52

mainly due to the chelation of the organic ligand with the Pd (II) ion.[55]

3.7 | *In vitro* cytotoxicity assays

Cytotoxicity assays of ligand and complexes were performed against two tumour cell lines, human cervical cancer cell line (HeLa) and human breast cancer cell line (MCF-7), using MTT assay. The results were analysed by means of cell inhibition expressed as (50% activity) IC_{50} values (concentration of compounds required to achieve 50% cell death) and are summarized in Table 6. From the biological assays of the ligand and Pd(II) complexes, the complexes exhibit more significant activities than the ligand against cancer cells, which confirms that the chelation of ligand with the Pd(II) ion is the only responsible factor for the observed cytotoxic properties of the new complexes.

TABLE 6 Cytotoxic activity of ligand and complexes against the HeLa and MCF-7 cancer cell lines

Compound	IC_{50} (μM)	
	HeLa	MCF-7
1	95.17	92.91
2	35.13	31.02
3	45.88	44.54
Cisplatin	16.21	15.35

The results indicate that both of the palladium complexes exhibit anti-tumour activities against the human cancer cell lines. The enhanced cytotoxic properties of the complexes over the ligand may be due to the extended planar structure induced by the $\pi \rightarrow \pi^*$ conjugation resulting from the chelation of the hydrazone ligand to the palladium ion in the complexes.[56] The *in vitro* cytotoxic activity studies indicate that the two complexes have better activities than the corresponding ligand but show significantly less activity than standard cisplatin. Finally, the observed ordering of the cytotoxicity among the two complexes is very similar to that of the DNA and BSA binding activities, showing the higher potential for complex **2**.

4 | CONCLUSIONS

In summary, a hydrazone ligand and its palladium(II) complexes were synthesized and characterized. The dibasic tridentate coordination of the ligand with central metal and the molecular structures of the ligand and both new complexes **2** and **3** were authenticated by X-ray diffraction studies. DNA binding of the ligand and Pd(II) complexes suggests that the two complexes bind to DNA more strongly than the ligand. The strong binding affinity of the complexes is attributed to the extension of the π system of the intercalated ligand which leads to a greater planar area of the complexes than the free ligand enabling the complexes to penetrate more deeply into, and stack more strongly with, the base pairs of DNA. In addition, the protein interaction properties of the new compounds were studied using UV–visible and fluorescence spectroscopies, and the results indicated that complex **2** has stronger binding compared with complex **3** and the ligand. The results obtained from three different antioxidant assays showed the significant efficacy in scavenging radicals and the assumed patterns of activity decreased in the following order: **2** > **3** > **1**. The cytotoxicity of the compounds against a panel of cancer cells demonstrated that the new complexes **2** and **3** showed promising tumour cell growth-inhibiting activity compared to the free ligand. Among the trivalent palladium hydrazone complexes, that containing triphenylphosphine as a co-ligand exhibited superior performance than its arsine-containing counterpart.

The outcome of this study would be helpful for understanding the mechanism of interactions of Pd(II) hydrazone complexes with serum albumin and nucleic acid and also in the development of potential probes for BSA and DNA structure and conformation, or new therapeutic agents for many diseases.

REFERENCES

[1] A. Jemal, F. Bray, M. Melissa, J. Ferlay, D. Forman, *CA Cancer J. Clin.* **2011**, *61*, 69.

[2] F. Bray, A. Jemal, N. Grey, J. Ferlay, D. Forman, *Lancet Oncol.* **2012**, *13*, 790.

[3] F. Arjmand, I. Yousuf, Y. Zaidi, L. Toupet, *RSC Adv.* **2015**, *5*, 16250.

[4] I. Meistermann, V. Moreno, M. J. Prieto, E. Moldrheim, E. Sletten, S. Khalid, P. M. Rodger, J. C. Peberdy, C. J. Isaac, A. Rodger, *Proc. Natl. Acad. Sci. U. S. A.* **2002**, *99*, 5069.

[5] V. Rajendiran, M. Murali, E. Suresh, S. Sinha, K. Somasundaram, M. Palaniandavar, *Dalton Trans.* **2008**, 148.

[6] E. Meggers, *Angew. Chem. Int. Ed.* **2011**, *50*, 2442.

[7] N. P. Barry, P. J. Sadler, *Chem. Commun.* **2013**, *49*, 5106.

[8] K. Zheng, F. Liu, X. M. Xu, Y. T. Li, Z. Y. Wu, C. W. Yan, *New J. Chem.* **2014**, *38*, 2964.

[9] M. Navarro, E. J. Cisneros-Fajardo, A. Sierralta, M. F. Mestre, P. Silva, D. Arrieche, E. Marcha, *J. Biol. Inorg. Chem.* **2003**, *8*, 401.

[10] F. Kratz, R. Muller-Driver, I. Hofmann, J. Drevs, C. Unger, *J. Med. Chem.* **2000**, *43*, 1253.

[11] D. Lu, X. Zhao, Y. Zhao, B. Zhang, B. Zhang, M. Geng, R. Liu, *Food Chem. Toxicol.* **2011**, *49*, 3158.

[12] J. E. Patterson, D. M. Geller, *Biochem. Biophys. Res. Commun.* **1977**, *74*, 1220.

[13] R. T. A. McGillivray, D. W. Chung, E. W. Davie, *Eur. J. Biochem.* **1979**, *98*, 477.

[14] J. Ruiz, N. Cutillas, C. Vicente, M. D. Villa, G. Lopez, J. Lorenzo, F. X. Aviles, V. Moreno, D. Bautista, *Inorg. Chem.* **2005**, *44*, 7365.

[15] S. Ray, R. Mohan, J. K. Singh, M. K. Samantaray, M. M. Shaikh, D. Panda, P. Ghosh, *J. Am. Chem. Soc.* **2007**, *129*, 15042.

[16] H. Daghriri, F. Huq, P. Beale, *Coord. Chem. Rev.* **2004**, *248*, 119.

[17] E. Gao, C. Liu, M. Zhu, H. Lin, Q. Wu, L. Liu, *Anti-Cancer Agents Med. Chem.* **2009**, *9*, 356.

[18] S. A. Abu-Surrah, M. Kettunen, *Curr. Med. Chem.* **2006**, *13*, 1337.

[19] A. C. Caires, *Anti-Cancer Agents Med. Chem.* **2007**, *7*, 484.

[20] A. S. Abu-Surrah, H. H. Al-Sadoni, M. Y. Abdalla, *Cancer Ther.* **2008**, *6*, 1.

[21] P. Souza, A. I. Matesan, in *Palladium: Compounds, Production and Applications*, (Ed: K. M. Brady), Nova Science Publishers, New York **2011**.

[22] A. I. Matesanz, C. Hernandez, A. Rodriguez, P. Souza, *J. Inorg. Biochem.* **2011**, *105*, 1613.

[23] P. Sathyadevi, P. Krishnamoorthy, M. Alagesan, K. Thanigaimani, P. Thomas Muthiah, N. Dharmaraj, *Polyhedron* **2012**, *31*, 294.

[24] S. Pal, J. Pushparaju, N. J. Sangeetha, S. Pal, *Transition Met. Chem.* **2000**, *25*, 529.

[25] Z. C. Liu, B. D. Wang, Z. Y. Yang, Y. Li, D. D. Qin, T. R. Li, *Eur. J. Med. Chem.* **2009**, *44*, 4477.

[26] J. L. Burmeester, F. Basolo, *Inorg. Chem.* **1964**, *3*, 1587.

[27] S. M. A. R. T. Siemens, *SAINT Area detector control and Integration software*, Siemens Analytical X-ray Instruments Inc., Madison, WI **1996**.

[28] G. M. Sheldrick, *SADABS, Program for empirical absorption correction of area detector data*, University of Gottingen **1997**.

[29] G. M. Sheldrick, *SHELXS-97, Program for the solution of crystal structures*, University of Gottingen, Germany **1997**.

[30] G. M. Sheldrick, *Acta Crystallogr.* **1900**, *46*, 467.

[31] A. Wolfe, G. H. Shimer, T. Meehan, *Biochemistry* **1987**, *26*, 6392.

[32] Y. Hua, Y. Liu, J. Wang, X. Xiao, S. Qu, *J. Pharm. Biomed. Anal.* **2004**, *36*, 915.

[33] M. S. Blois, *Nature* **1958**, *181*, 1199.

[34] T. Nash, *J. Biochem.* **1953**, *55*, 416.

[35] L. C. Green, D. A. Wagner, J. Glogowski, P. L. Skipper, J. S. Wishnok, S. R. Tannenbaum, *Anal. Biochem.* **1982**, *126*, 131.

[36] T. J. Mosmann, *J. Immunol. Methods* **1983**, *65*, 55.

[37] A. R. B. Rao, S. Pal, *J. Organomet. Chem.* **2013**, *731*, 67.

[38] D. X. West, I. S. Billeh, J. P. Jasinski, J. M. Jasinski, R. J. Butcher, *Transition Met. Chem.* **1998**, *23*, 209.

[39] P. B. Sreeja, M. R. P. Kurup, *Spectrochim. Acta* **2005**, *61*, 331.

[40] Y. P. Tiam, C. Y. Duan, Z. L. Lu, X. Z. You, *Polyhedron* **1996**, *15*, 2263.

[41] E. W. Ainscough, A. M. Brodie, A. J. Dobbs, J. D. Ranford, J. M. Waters, *Inorg. Chim. Acta* **1998**, *267*, 27.

[42] F. Basuli, M. Ruf, C. G. Pierpont, S. Bhattacharya, *Inorg. Chem.* **1998**, *37*, 6113.

[43] P. Sathyadevi, P. Krishnamoorthy, N. S. P. Bhuvanesh, P. Kalaiselvi, V. Vijaya Padma, N. Dharmaraj, *Eur. J. Med. Chem.* **2012**, *55*, 420.

[44] K. Sampath, S. Sathiyaraj, C. Jayabalakrishnan, *Spectrochim. Acta* **2013**, *105*, 582.

[45] E. Ramachandran, D. S. Raja, N. P. Rath, K. Natarajan, *Inorg. Chem.* **2013**, *52*, 1504.

[46] B. V. Rosenberg, L. Camp, T. Krigas, *Nature* **1965**, *205*, 698.

[47] S. Arounaguiri, B. G. Maiya, *Inorg. Chem.* **1999**, *38*, 842.

[48] T. Sathiya Kamatchi, N. Chitrapriya, H. Lee, C. F. Fronczek, F. R. Fronczekc, K. Natarajan, *Dalton Trans.* **2012**, *41*, 2066.

[49] B. D. Wang, Z. Y. Yang, Q. Wang, T. K. Cai, P. Crewdson, *Bioorg. Med. Chem.* **2006**, *14*, 1880.

[50] J. Pratihar, N. Maiti, P. Pattanayak, S. Chattopadhyay, *Polyhedron* **2005**, *24*, 1953.

[51] E. S. Koumousi, M. Zampakou, C. P. Raptopoulou, V. Psycharis, C. M. Beavers, S. J. Teat, G. Psomas, T. C. Stamatatos, *Inorg. Chem.* **2012**, *51*, 7699.

[52] C. Tan, J. Liu, H. Li, W. Zheng, S. Shi, L. Chen, L. Ji, *J. Inorg. Biochem.* **2008**, *102*, 347.

[53] Y. Wang, H. Zhang, G. Zhang, W. Tao, S. Tang, *J. Lumin.* **2007**, *126*, 211.

[54] H. Y. Liu, Z. H. Xu, X. H. Liu, P. X. Xi, Z. Z. Zeng, *Chem. Pharm. Bull.* **2009**, *57*, 1237.

[55] M. Mohanraj, G. Ayyannan, G. Raja, C. Jayabalakrishnan, *J. Photochem. Photobiol.* **2016**, 158,164.

[56] M. Alagesana, N. S. P. Bhuvanesh, N. Dharmaraj, *Eur. J. Med. Chem.* **2014**, *78*, 281.

SUPPORTING INFORMATION

Additional supporting information can be found in the online version of this article at the publisher's website.

How to cite this article: Ayyannan, G., Veerasamy, P., Mohanraj, M., Raja, G., Manimaran, A., Velusamy, M., Bhuvanesh, N., Nandhakumar, R., and Jayabalakrishnan, C. (2016), Biological evaluation of organometallic palladium(II) complexes containing 4-hydroxybenzoic acid (3-ethoxy-2-hydroxybenzylidene)hydrazide: Synthesis, structure, DNA/protein binding, antioxidant activity and cytotoxicity, *Appl. Organometal. Chem.*, doi: 10.1002/aoc.3599